Biochimica et Biophysica Acta 1852 (2015) 2494–2503

Contents lists available at ScienceDirect

Biochimica et Biophysica Acta

journal homepage: www.elsevier.com/locate/bbadis

Activated STING enhances Tregs infiltration in the HPV-related carcinogenesis of tongue squamous cells via the c-jun/CCL22 signal

Liang Ding [a], Xiao-Feng Huang [a], Guan-Jun Dong [a], Er-Ling Hu [a], Sheng Chen [a], Ting-Ting Wang [a], Qin-Gang Hu [a], Yan-Hong Ni [a,*], Ya-Yi Hou [a,b,**]

[a] The State Key Laboratory of Pharmaceutical Biotechnology, Division of Immunology and Hospital of Stomatology, Medical School, Nanjing University, Nanjing, China
[b] Jiang su Key Laboratory of Molecular Medicine, Nanjing 210093, China

ARTICLE INFO

Article history:
Received 31 March 2015
Received in revised form 7 July 2015
Accepted 19 August 2015
Available online 21 August 2015

Keywords:
STING
c-jun
miR-27
HPV
Tregs

ABSTRACT

The negative role of the activated stimulator of IFN genes (STING) has been uncovered in autoinflammatory disease and cancer. However, the role of STING in virus-related carcinogenesis is not well known. Herein, HPV^{+} tongue squamous cell carcinoma (TSCC) (n = 25) and HPV^{-} TSCC samples (n = 25) were randomly collected and were verified by in situ hybridization (ISH) and p16 immunohistochemistry (IHC) to assess the expression and activated status of STING through IHC. The results showed that the expression of STING was up-regulated during the development of TSCC. Interestingly, although the expression of STING showed no difference between $HPV^{+/-}$ TSCC samples, the activated status of STING with dark staining around the nucleus was observed in HPV^{+} TSCC samples. The role of activated STING was analyzed in three cell lines by siRNA and indicated that activated STING had no impact on cell viability or apoptosis but promoted the induction of several immunosuppressive cytokines, e.g., IL-10, IDO and CCL22, which facilitated the infiltration of regulatory T cells (Tregs). Moreover, increased infiltration of $Foxp3^{+}$ Tregs along with increased expression of CCL22 was confirmed in HPV^{+} TSCC samples. An inhibitor of the MAPK/AP-1 pathway (U0126) and the silencing of c-jun significantly suppressed CCL22 induction and the recruitment of Tregs by activated STING. Furthermore, down-regulated miR-27 was verified in independent fresh TSCC samples (n = 50) and eight cell lines, which enhanced STING activation and led to increased CCL22 expression for Tregs recruitment in the TSCC microenvironment. Therefore, our findings provided distinct insight into the side effects of activated STING in HPV-related carcinogenesis.

1. Introduction

Stimulator of interferon genes (STING), also known as TMEM173, predominantly resides in the endoplasmic reticulum and mitochondrial-associated membrane [1] and serves as a critical adaptor that detects dsDNA from viral and eukaryotic pathogens as well as cyclic dinucleotide (CDN) from bacteria [2]. Currently, CDN and human endogenous messenger 2′-5′, 3′-5′cyclic AMP-GMP (2′-3′cGAMP) have immunostimulatory properties and are candidates for a vaccine adjuvant based on STING activation [3]. 2′-3′cGAMP is generated by cyclic GMP-AMP synthase (cGAS), which directly binds dsDNA. Once STING senses dsDNA or 2′-3′ cGAMP in the cytoplasm, it relocates to cytoplasmic punctate structures around the nucleus and induces potent anti-viral genes and other proinflammatory cytokines to participate in anti-infection immunity or autoimmune functions [4,5]. STING-associated vasculopathy with onset in infancy (SAVI) was reported to be an autoinflammatory disease caused by mutant STING, which was, clinically, a gain-of-function mutation [6]. Interestingly, an unexpected negative regulatory role for STING had been reported in that STING could inhibit unchecked immune activation during systemic lupus erythromatous (SLE), and STING-deficient SLE mice had significantly increased autoantibody production and significantly reduced percentages of activated regulatory T cells (Tregs) cells in axillary lymph nodes as well as shorter lifespans than controls [7]. However, the exact mechanism of the relationship between STING and Tregs needs to be elucidated.

Recently, STING was reported to be a double-edged sword for non-virus-related oncoimmunology [4,8,9]. On the one hand, in a colorectal tumorigenesis mouse model, colons of STING-deficient mice were susceptible to colitis-associated colorectal cancer and exhibited significant intestinal damage and proliferation during early stages of carcinogenesis [9]. On the other hand, STING was found to promote inflammation-driven skin carcinogenesis by enhancing inflammatory cytokine levels of the infiltrating phagocytes, but the $STING^{-/-}$ mice were resistant to mutagen-induced skin carcinogenesis compared to wild-type mice [4].

* Correspondence to: Y. H. Ni, Central Laboratory, Hospital of Stomatology and the State Key Laboratory of Pharmaceutical Biotechnology, Division of Immunology, Medical School, Nanjing University, Nanjing 210008, China.
** Correspondence to: Y. Y. Hou, The State Key Laboratory of Pharmaceutical Biotechnology, Division of Immunology, Medical School, Nanjing University, Nanjing 210093, China.
E-mail addresses: niyanhong12@163.com (N. Yan-Hong), yayihou@nju.edu.cn (H. Ya-Yi).

http://dx.doi.org/10.1016/j.bbadis.2015.08.011
0925-4439/

Additionally, Mellor et al. found that selective STING activation could suppress experimental autoimmune encephalitis (EAE) in an IDO-dependent manner, which implicated STING as being versatile in the manipulation of the immune balance [10].

Human papillomaviruses (HPVs) are small double-stranded DNA (dsDNA) viruses that infect squamous epithelia. Viral persistence followed by HR-HPV infection, particularly HPV-16, 18, is a key risk factor for carcinogenesis [11]. Of note, because HPVs are difficult to culture in vitro and because of the insufficiency of mouse models, research on the natural infection history of HPVs is very difficult [12], and the exact molecular evidence for the role of HPVs in relative cancers is limited. Other than its viral protein E6/7, many reports have indicated that HPV infection could change the status of the host immune system [13]. High infiltration of $Foxp3^+$ Tregs is often associated with an immunosuppressive microenvironment and promotes the progression of tumors. A higher percentage of $Foxp3^+$ Tregs was observed in HPV^+ tonsillar cancer patients [14]. Badoual et al. showed that HPV^+ head and neck cancers were more heavily infiltrated by $Foxp3^+$ Tregs [15], and studies on cervical cancer also showed increasing levels of Foxp3 mRNA and $Foxp3^+$ Tregs infiltration in HPV^+ tumors with unclear molecular mechanisms [16,17].

New cancer statistics show that tongue squamous cell carcinoma (TSCC) is still the most common oral cancer [18]. Although HPV integration is important for carcinogenesis, episomal HPV DNA has also been detected in some carcinomas, suggesting that the episomes may induce malignant progression [19]. Thus, we hypothesized that HPV infection could be sensed by DNA sensors to activate STING, contributing to the infiltration of $Foxp3^+$ Tregs and promoting the establishment and maintenance of the TSCC microenvironment.

2. Materials and methods

2.1. Patients and tissue samples

In this study, HPV^+ TSCC samples ($n = 25$) and HPV^- TSCC samples ($n = 25$) were collected to assess the expression and activated status of STING, and 50 fresh tissue samples collected from surgery were used for microRNA analysis. All of the patients diagnosed with primary TSCC were confirmed by hematoxylin and eosin staining by experienced pathologists from the Department of Pathology at Nanjing Stomatology Hospital between 2003 and 2011, and ethical approval for this study was obtained from the Research Ethics Committee of Nanjing Stomatology Hospital. The HPV status was confirmed by in situ hybridization (ISH) and p16 immunohistochemistry (IHC) (HPV testing and the patient information are available upon request). Patients who were diagnosed with autoimmune or other malignant diseases and pregnant or lactating individuals were excluded from our experimental group. No patients underwent preoperative chemotherapy and/or radiotherapy. All of the TSCC tissues were evaluated according to WHO classifications by two pathologists.

2.2. Immunohistochemistry and immunofluorescence assays

Immunohistochemistry and immunofluorescence assays are described in the supplementary materials and methods.

2.3. Cell culture and reagents

The normal human keratinocyte line HaCaT and the oral squamous cell carcinoma cell lines HSC-3, Scc-4, Scc-1, HB, Scc-14a, Scc-14b, OSCC-3, and Cal-27 were cultured in Dulbecco's Modified Eagle's medium supplemented with 10% FBS (Life Technologies, USA) at 37 °C, 5% CO_2 conditions. Detailed information on the antibodies and reagents used in this study is provided in Supplementary Table S3.

2.4. siRNA transfection and cell viability assay

HaCaT, HSC-3 and Scc-4 cells were seeded in 96-well plates at 5000 cells/well. After the initial transfection of siRNA or negative controls were place in each well, cells were cultured for 48 h and then transfected with poly (dA: dT) for 10 h. Cell counting kit-8 (Kumamoto, Japan) was used for cell viability assay, and the absorbance was measured at 450 nm by a microplate reader.

2.5. RNA isolation and qRT-PCR

Fresh tissue samples ($n = 50$) or cell lines were collected. According to the standard RNA isolation protocol, total RNA was extracted using Trizol reagent (Invitrogen). Quantitative real-time RT-PCR (qRT-PCR) was performed, and the expression levels were normalized to GAPDH for gene expression or U6 for microRNA expression.

2.6. Flow cytometry assay

For the apoptosis analysis, 2 μl of annexin V mixed with 2 μl of propidium iodide (PI, eBioscience) were added into each tube for 30 min. For the Tregs analysis, FITC-anti-human CD4 (Cat No. 555346, BD Pharmingen™), PE-$Foxp3^+$ (Cat No. 560046, BD Pharmingen™) and APC-anti-human CD25 (Cat No. 555434, BD Pharmingen™) were used to mark Tregs according to the manufacturer's instructions and quantified by flow cytometry on a FACS Calibur instrument.

2.7. Preparation of cell extracts and immunoblotting

Prepared cells for western blots were collected with PBS and then lysed in RIPA buffer with protease inhibitors and phosphatase inhibitors (Roche Applied Science). Detailed procedures for immunoblotting are described elsewhere [20].

2.8. ELISA

Cells were transfected with siRNA, followed by transfection with poly(dA:dT) or 2′-3′ cGAMP for the indicated time, and then, the supernatants were collected for the measurement of CCL22 with a MDC (CCL22) human ELISA kit (Cat No. ab100591, Abcam, USA) according to the manufacturer's instructions.

2.9. Luciferase assay

HSC-3 cells were transfected with siRNA and reporter plasmid (CCL22-luc) for 24 h. Subsequently, a second transfection of poly (dA: dT) or 2′-3′ cGAMP was performed for 10 h. Then, the cells were collected and a luciferase assay was performed using a Dual-Luciferase Reporter Assay System (Promega).

2.10. Separation of peripheral blood mononuclear cells and the migration assay

Approximately 100 ml of fresh peripheral blood from healthy donors was collected, and PBMCs were separated by lymphocyte separation medium according to the manufacturer's instructions. For the cell migration assay, 12-well plates were used, 500 μl of cell supernatant was added to the lower chamber and two million human PBMCs were added to the upper chamber of the inserts with a 5-μm pore size (Cat No. PIMP15R48, Millipore). In some experiments, 7 μg/ml of anti-CCL22 neutralizing antibodies (Cat No. ab9847, Abcam, USA) or the MAPK inhibitor U0126 (Cat No. S1801, Beyotime) were added to the lower compartment. After migration for 8 h, cells from the lower compartment were collected and Tregs was analyzed by flow cytometry.

2.11. Statistical analyses

Statistical analyses were performed using the Statistical Package for Social Sciences version 16.0 (SPSS 16.0, SPSS Inc., Chicago, IL, USA) and the Prism statistical software package (version 5.0, Graphpad Software Inc.). Unpaired t-tests or Mann–Whitney U tests were used to compare the two groups, and the differences between more than two groups were analyzed by the Kruskal–Wallis test. Each experiment was repeated at least three times. Differences were considered statistically significant when $P < 0.05$.

3. Results

3.1. The expression of STING is increased in TSCC samples, and HPV$^+$ TSCC samples contain the activated status of STING

HPVs are difficult to culture in vitro, which makes it harder to investigate its natural infection history with a mouse model. Thus, the exact molecular evidence for the role of HPV infections in relative cancers is limited. To evaluate the hypothesis that STING associates with HPV infection to promote tumor formation, we first investigated the expression of STING in TSCC patients. The results of IHC analysis showed that STING expression showed negative immunostaining in the relative normal epithelial tissue, weak positive staining in the dysplasia tissue and strong positive staining in the whole sample. Of note, STING immunostaining exclusively occurred in the cytoplasm (Fig. 1A). Moreover, STING expression was significantly upregulated in the tumor, with an immunohistochemistry (IHC) intensity score over 2 (++) in 31 of 50 TSCC samples, while rare positive staining was detected in relatively normal epithelial tissue with an IHC intensity score less than 1 (+) in 43 of 50 TSCC samples (Fig. 1B). STING expression in distinct microlocalization was also statistically analyzed (Supplementary Table S1). A previous study showed that the presence of high-risk HPV reduces STING and IFN-κ via its viral protein E2 for immune evasion in cervical cancer [21]. However, we should note that the E2 proteins are expressed at early stages of the viral life cycle and have a very short half-life (full-length BPV1 E2 has a half-life of 40 min) [22]. Interestingly, our results showed that HPV$^-$ and HPV$^+$ TSCC patients showed a similar STING expression. Thus, we hypothesize that at the early stage of infection, HPV took advantage of E2 to avoid immune surveillance, but at the advanced stage of infection, the E2 proteins were significantly downregulated to restore STING expression; therefore, HPV infection activated and utilized STING to participate into the formation and progression of cancer (Fig. 1C).

However, it is known that STING executes anti-infection immunity through dimerization to activate and relocate to cytoplasmic punctate structures around the nucleus via dsDNA in the cytoplasm [20,23]. Thus, the status of STING activation was examined. Strikingly, dark staining around the nucleus was found in 16 of 25 HPV$^+$ TSCC samples, while diffuse staining over the whole cytoplasm was found in 22 of 25 HPV$^-$ TSCC samples (Fig. 1D and E). The phenomena were in agreement with previous reports that stated that STING translocated from the ER or mitochondria to cytoplasmic punctate structures around the nucleus in response to dsDNA in vitro [23]. The results of these analyses revealed a high correlation between HPV infection and STING activation, suggesting that activated STING may be a potential factor in predisposing patients with a HPV infection to accelerating the progression of TSCC.

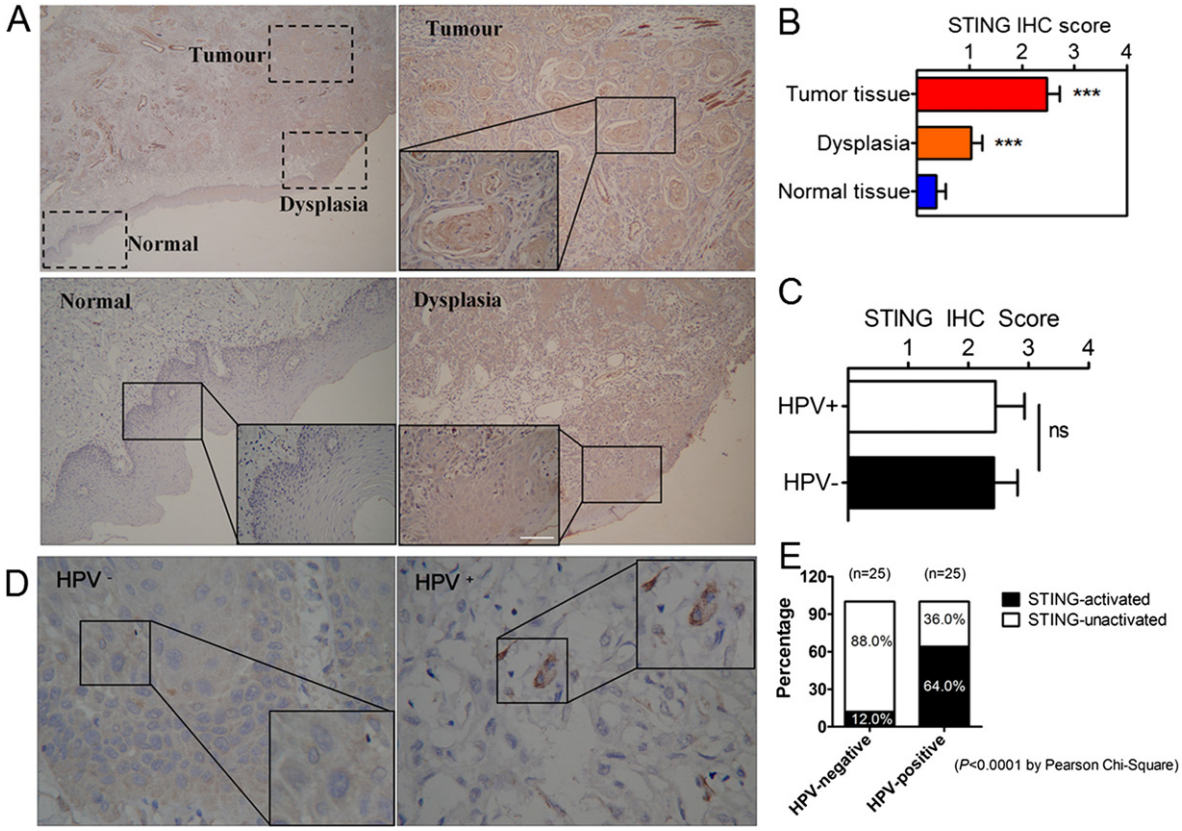

Fig. 1. Activated STING is associated with the HPV infection status in TSCC patients. (A) The expression of STING in TSCC (n = 50) was performed by IHC analysis via an anti-STING antibody, diluted × 100. Relatively normal tissues, dysplasia tissues and tumor tissue are shown in each dashed box. Scale bar, 150 μm. (B) The IHC scores of STING were assessed in normal tissues, dysplasia and tumor tissue or (C) in HPV$^+$ and HPV$^-$ groups. (***P < 0.001, the P-value was determined by the Kruskal–Wallis test). (D) Distinct status of STING in HPV+ and HPV− groups. Left: IHC of the HPV− groups showed an inactivated status of STING. Right: IHC of the HPV$^+$ groups showed an activated status of STING. Scale bar, 50 μm. (E) The percentage of activated STING in HPV-positive TSCC patients compared with HPV-negative TSCC patients was analyzed.

3.2. Activated STING does not influence cell viability or apoptosis in TSCC

To investigate the possible mechanisms of activated STING in the carcinogenesis of HPV^{+} TSCC patients, we first assessed the effects of STING on cell death. Currently, the correlation between STING and cell death has been reported by a few studies. B-cell lymphoma 2 (Bcl2)-associated X protein is a pro-apoptotic molecule and ethanol-induced ER stress triggers hepatocyte apoptosis by the IRF3-Bax pathway, which is dependent on STING [24]. Another study indicated that STING overexpression, but not activation, leads to cell death by activating caspases in breast cancer cell lines [25]. Liu et al. showed that when endothelial cells from human umbilical veins were stimulated with cGAMP, the expression of inducible nitric oxide synthase, E-selectin, and tissue factors were up-regulated and induced endothelial cell death [6].

We took advantage of polydeoxyadenine-polydeoxythymidine, poly (dA: dT), as a mimic stimulator of dsDNA from HPV to activate STING, which was similar to the bacterial and virus dsDNA that could be sensed by STING and dimerized for activation [5]. Because HPV can infect normal epithelial cells and cancer cells under natural circumstances [26], poly (dA: dT) transfection was performed on one normal epithelial cell line and two TSCC cell lines. After the transfection of poly (dA:

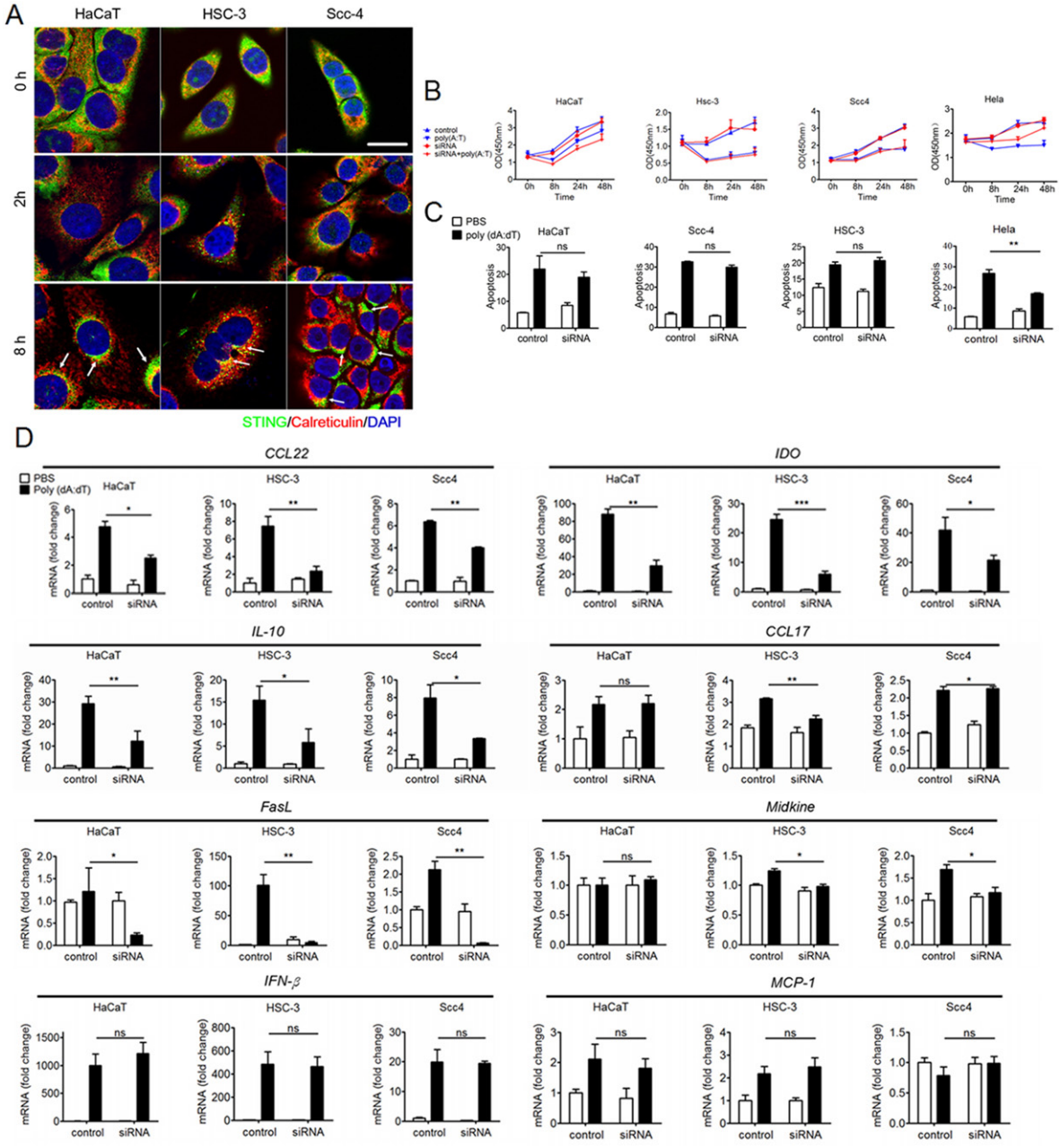

Fig. 2. STING activation has no effect on the cell viability or apoptosis of TSCC but promotes the secretion of immunosuppressive cytokines. (A) HaCaT, HSC-3 and Scc-4 cells were seed in 24-well plates and transfected with 4 μg/ml poly (dA: dT) for the indicated time and immunostained with the indicated antibodies. Double staining was used; STING is green, and calreticulin (ER marker) is red. Scale bar, 10 μm. (B) Three cell lines and HeLa were transfected with 50 nM STING siRNA or negative control for 48 h and then transfected with 4 μg/ml poly (dA:dT) or PBS for the indicated time, and cell viability was measured by the CCK-8 assay. (C) Cells were treated as in C, apoptosis was analyzed by a flow cytometry assay. The *P*-value was calculated by Student's *t*-test. Activated STING promotes the secretion of immunosuppressive cytokines. (D) qRT-PCR validates the expression changes of cytokines and its ligands by STING activation, including CCL22, IDO, IL-10, FasL, MK, IFN-β and MCP-1 ($^{*}P < 0.05$, $^{**}P < 0.001$, $^{***}P < 0.001$ by Mann Whitney *U* test). Data represent the means ± s.d. Data represent the means ± s.d.

dT), we observed that STING migrated from the endoplasmic reticulum (ER) to perinuclear regions and was activated in response to cytoplasmic dsDNA ligands in three cell lines (Fig. 2A). Considering that poly (dA:dT) could trigger multiple pathways, including retinoic acid inducible gene/RIG-like receptors (RLRs), additional transient transfections of siRNA-STING or control siRNA (Supplementary Fig. S1) were used to confirm its function after poly (dA:dT) stimulation for 0 h, 8 h, 24 h and 48 h, but we found that STING activation had no impact on the cell viability and apoptosis of HaCaT, HSC-3 and SCC-4 (Fig. 2B and C).

To provide further support for the specific role of STING activation in TSCC, the HeLa cervical cancer cell line, which is also frequently associated with HPV, was examined as above. Surprisingly, STING activation inhibited the cell viability and promoted apoptosis (Fig. 2B and C). Therefore, these results indicate that STING may exert its pro-apoptotic function in a tumor type-dependent manner.

3.3. Activated STING enhances the secretion of cytokines, including CCL22, IDO and IL-10 in TSCC

Because STING shows no impact on cell viability or apoptosis, we investigated the role of activated STING in the establishment of the tumor microenvironment. We focused on the cell's nonautonomous route for STING to promote the depravation of oral lesions. Of note, STING activation highly induced the expression of cytokines, including CCL22, IDO and IL-10, in all three cell lines (Fig. 2D, Supplementary Table S2). The chemokine CCL22 can recruit Foxp3$^+$ Tregs via CCR4 in many types of cancer tumor microenvironments [27]. The up-regulated expression of IDO and IL-10 also can induce Tregs expansion and is associated with a particularly unfavorable clinical outcome [28]. In addition, although CCL17 could also recruit Tregs, its expression was not affected by STING activation in HaCaT or SCC4 (Fig. 2D). Tumor cells secrete Fas ligand (FasL) to avoid immune surveillance. The up-regulated FasL mRNA level was observed in three cell lines in response to dsDNA (Fig. 2D). Midkine (MK) is a pleiotropic growth factor that is often overexpressed in many cancers [29], and we found that STING activation significantly increased the MK mRNA in TSCC cell lines other than the HaCaT cell line (Fig. 2D). The levels of interferon-β (IFN-β) and monocyte chemotactic protein-1 (MCP-1) were reported to be up-regulated by STING activation in mouse embryonic fibroblasts (MEFs) [30], but no change was observed in the normal or TSCC cells by RNAi knockdown of STING, which implied that there were other potential pathways to induce IFN-β or MCP-1 (Fig. 2D). However, the level of IFN-β mRNA was up-regulated as previously reported in the HeLa cell line (Supplementary Fig. S2). Other tumor-related cytokines or receptors were also examined, such as vascular endothelial growth factor (VEGF), macrophage inflammatory protein-1α (MIP-1α), matrix metallopeptidase 9 (MMP-9), Fas or IFNAR1. However, no consistent results were observed in HaCaT, HSC-3 and Scc-4 cells (Supplementary Table S2). These results indicated that STING activation promoted the secretion of cytokines, including CCL22, IDO and IL-10, which might be key driving factors in the development of HPV$^+$ TSCC.

3.4. Activated STING promotes the recruitment of Tregs by up-regulating CCL22 in HPV$^+$ TSCC patients

Our in vitro data revealed that STING activation could induce CCL22 expression, which had the ability to recruit Foxp3$^+$ Tregs. To establish clinical evidence of the relationship between STING activation and Foxp3$^+$ Tregs recruitment in HPV$^+$ TSCC, immunohistochemical staining of FoxP3$^+$ on the same set of tissue specimens was performed and analyzed (Fig. 3A). Unsurprisingly, the infiltration of FoxP3$^+$ Tregs in tumor stroma was observed more frequently in HPV$^+$ TSCC patients than in HPV$^-$ TSCC patients (Fig. 3B). Correspondingly, the amount of FoxP3$^+$ Tregs was significantly higher in the STING-activated group than in the STING-inactivated group (Fig. 3C). We further examined the role of CCL22 in the recruitment of Tregs in the clinic. Of note, the immunohistochemistry results showed that the CCL22 immunostaining was consistent with FoxP3$^+$ immunostaining in TSCC samples. Specifically, the increased expression of CCL22 in tumor sections was exhibited in HPV$^+$ TSCC patients and the STING-activated group (Fig. 3D–F). These data suggest that STING may be activated to promote the infiltration of Tregs into the stroma by inducing CCL22 expression during the detection of the dsDNA of HPV. These results demonstrated that the highly up-regulated Tregs/CCL22 chemokine axis in the STING-activated TSCC group promoted immunosuppression and participated in the development of HPV$^+$ TSCC.

3.5. c-Jun is required for elevated levels of CCL22 by STING activation

Currently, there are no effective and targeted therapies for cancer patients with a HPV infection. The molecular mechanism of CCL22 induction by STING activation could provide a better understanding of the progression of HPV$^+$ TSCC and help to identify an effective therapeutic target. The activation of NF-κB, AP-1 and Jak/STAT is known to induce the gene expression of many chemokines. Thus, we examined the effects of inhibitors of the NF-κB pathway (PTDC), MAPK/AP-1 pathway (U0126) and Jak/STAT pathway (AG490) on CCL22 induction by STING. The results showed that these inhibitors significantly suppressed both the phosphorylation of their independent target protein (Fig. 4A) and CCL22 expression induced by poly (dA: dT) (Fig. 4B).

There is a possibility that poly (dA: dT) may strongly activate many cytosolic pathways other than the STING-related pathway to produce CCL22. To exclude this possibility, a strong agonist of STING, 2′-3′ cGAMP, was used. Transfection of 2′-3′ cGAMP induced STING activation (Fig. 4C) and IFN-β production in normal epithelial cells and TSCC cells (Fig. 4D). The level of CCL22 induced by 2′-3′ cGAMP was almost abrogated by STING knockdown (Fig. 4E). However, the expression of CCL22 was significantly suppressed by U0126 other than PTDC or AG490 (Fig. 4 F). These results demonstrate that STING activation up-regulated the expression of CCL22 preferentially via the MAPK/AP-1 pathway, but not the NF-κB pathway or Jak/STAT pathway.

To verify our findings, c-Jun and c-Fos, the critical elements of AP-1 complexes [31], were analyzed. The results showed that STING activation increased the phosphorylation of c-Jun and c-Fos together with CCL22 production in a time-dependent manner (Fig. 4G). Interestingly, the silencing of c-Jun, but not c-Fos, remarkably inhibited the mRNA and protein induction of CCL22 (Fig. 4H–J). To provide further support for the role of AP-1 in the CCL22 production by STING activation, we next investigated the transcriptional activity of c-Jun and c-Fos by the luciferase assay. We found that c-Jun strongly promoted the initiation of the gene transcription of CCL22, while c-Fos had no effect (Supplementary Fig. S3). Together, these results implied that c-Jun was essential for the CCL22 production induced by STING activation and that the c-Jun inhibitor could be a potential clinical protocol for the treatment of HPV$^+$ TSCC patients.

3.6. miR-27 targeted STING and affected CCL22 expression and Tregs recruitment

Because of the immunosuppressive function of activated STING in HPV$^+$ TSCC, the mechanism to control the extent and strength of STING activation needed to be explored. Dysregulated miRNAs play a role in almost all aspects of cancer biology, such as angiogenesis, invasion/metastasis, apoptosis, proliferation, and the microenvironment [32]. Thus, several predicted microRNAs (miRNAs) that directly target the 3′ untranslated region (UTR) of STING were screened by miRWalk (http://www.umm.uni-heidelberg.de/apps/zmf/mirwalk/). Comparative analysis by 5 prediction programs were used to confirm the accuracy of the prediction; 12 predicted miRNAs which play important roles in cancer were selected, and their levels were determined in normal epithelial, dysplasia and tumor tissues from fresh tissues of TSCC patients ($n = 50$). The results showed that five miRNAs levels, including miR-

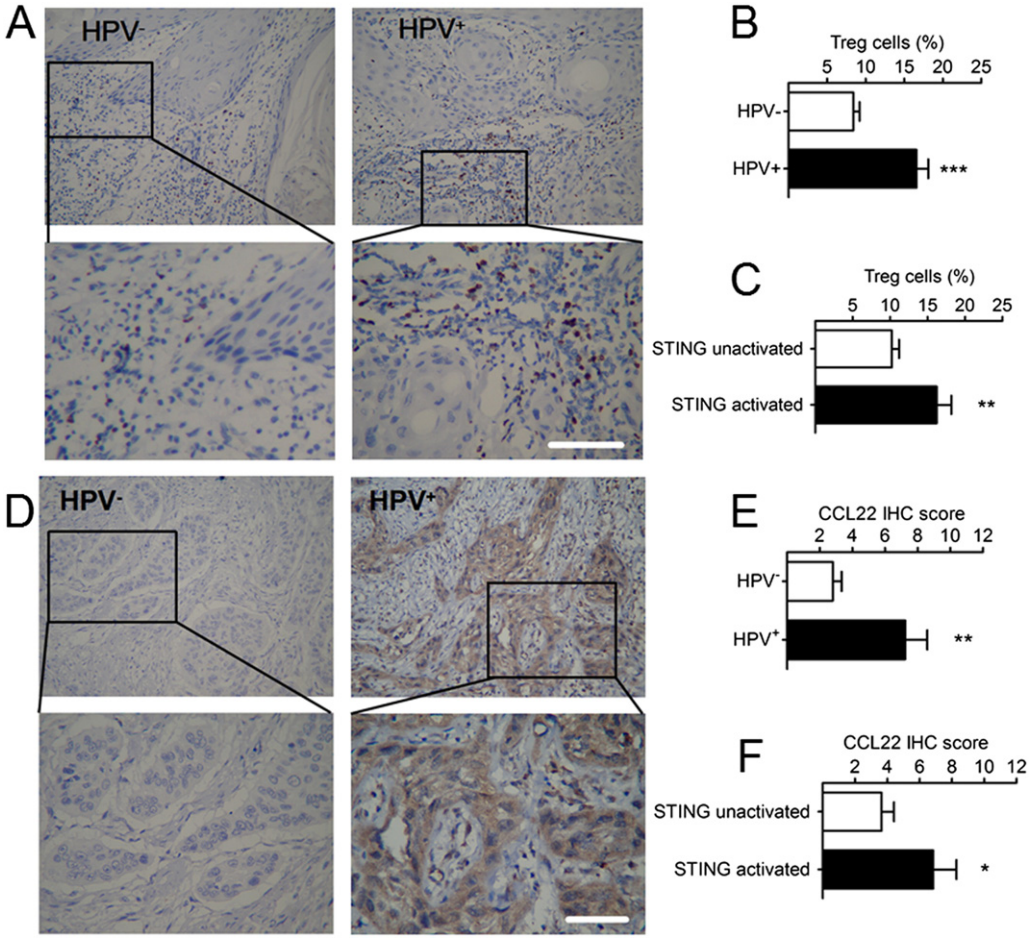

Fig. 3. The presence of CCL22/Tregs correlates with the poor prognosis of TSCC patients. (A) Foxp3-positive Tregs were determined by immunohistochemical staining via an anti-Foxp3 antibody (B) in HPV^+ and HPV^- groups, $^*P < 0.05$, the *P*-value was determined by an unpaired Student's *t*-test. (C) The IHC score of Foxp3-positive Tregs was also assessed in STING-inactivated and -activated groups ($^*P < 0.05$, the *P*-value was determined by an unpaired Student's *t*-test). (D–F) Similarly, CCL22 was also determined by IHC in the HPV^+ and HPV^- groups and in STING-inactivated and activated groups ($^*P < 0.05$, $^{***}P < 0.001$ by *t*-test).

27a, miR-27b, miR-124, miR-34c and miR-449b, presented gradually down-regulated trends from normal tissue to cancerous tissue, suggesting a correlation of the miRNAs with the up-regulation of STING (Fig. 5A). Moreover, according to the widely different expression of miRNAs in normal tissue, miR-27a/b was found to be the most significantly abundant among the miRNAs in normal tissue (Fig. 5B), and the ratio of miR-27a/miR-27b was 3:1. Therefore, we next determined the possibility that STING served as a target of miR-27a/b. The putative targeting sequences in the 3′UTR of STING predicted by TargetScan (http://www.targetscan.org) showed that the two miRNAs have the same target sites. We found that the enforced expression of miR-27 (miR-27a: 27b = 3:1, the mimic of natural expression ratio) reduced both STING mRNA and protein expression in the TSCC cell line (Fig. 5C). Meanwhile, one normal epithelial cell line and seven TSCC cell lines were examined by qPCR analysis, and the results showed that the level of miR-27a/b was reduced in most cancer cell lines. Correspondingly, STING expression in the TSCC cells was generally increased compared to the normal cell line (Fig. 5D). These data indicated that miR-27 was involved in the regulation of STING expression in TSCC cell lines.

We hypothesized that miR-27 could impair STING activation-induced CCL22 to recruit Tregs infiltration. To test the hypothesis, HSC-3 cells were transfected with miR-27 (miR-27a: miR-27b = 3:1), and then, STING was activated by poly (dA: dT) or 2′-3′ cGAMP. The results revealed that miR-27 effectively suppressed both CCL22 mRNA and protein levels (Fig. 5E). Moreover, the peripheral blood mononuclear cells (PBMCs) that were freshly isolated from healthy donors were treated with the indicated culture media from HSC-3 for the transwell assay (Fig. 5F), and $FoxP3^+CD4^+CD25^+$ Tregs were analyzed. Expectedly, STING activation promoted the migration of Tregs, while overexpression of miR-27 decreased the migratory activity of Tregs. Furthermore, an anti-CCL22 neutralizing antibody and the inhibitor of the MAPK/AP-1 pathway (U0126) significantly impaired the Treg cell migratory activity (Fig. 5G). These data indicated that the down-regulated miR-27 contributed to the increased CCL22 and Tregs recruitment via the enhancement of STING activation in HPV^+ TSCC.

4. Discussion

The scarcity of the HPV infection-mouse model limited the investigations on its complex mechanisms of carcinogenesis. Apart from its viral protein, in this study, we provided new clues regarding HPV infections in carcinogenesis and dissected the role of activated STING in the establishment of the HPV^+ TSCC microenvironment and found that HPVs hijack STING to induce CCL22 to recruit Tregs and that the down-regulated miR-27 amplifies the interaction among STING/CCL22/Tregs in the carcinogenesis of HPV^+ TSCC patients and brings the dark side of STING in cancer to light (Fig. 6).

Recently, more than 10 DNA sensors have been found to connect with the DNA sensing and immune defense, including Toll-like receptors (TLRs), RIG-like receptors (RLRs), NOD-like receptors (NLRs) and the enzyme cyclic GMP-AMP synthase (cGAS). As a newly discovered molecule in DNA sensing, the activation of the STING-IFN pathway is critical to limit the replication of DNA viruses, including HIV or HSV-1

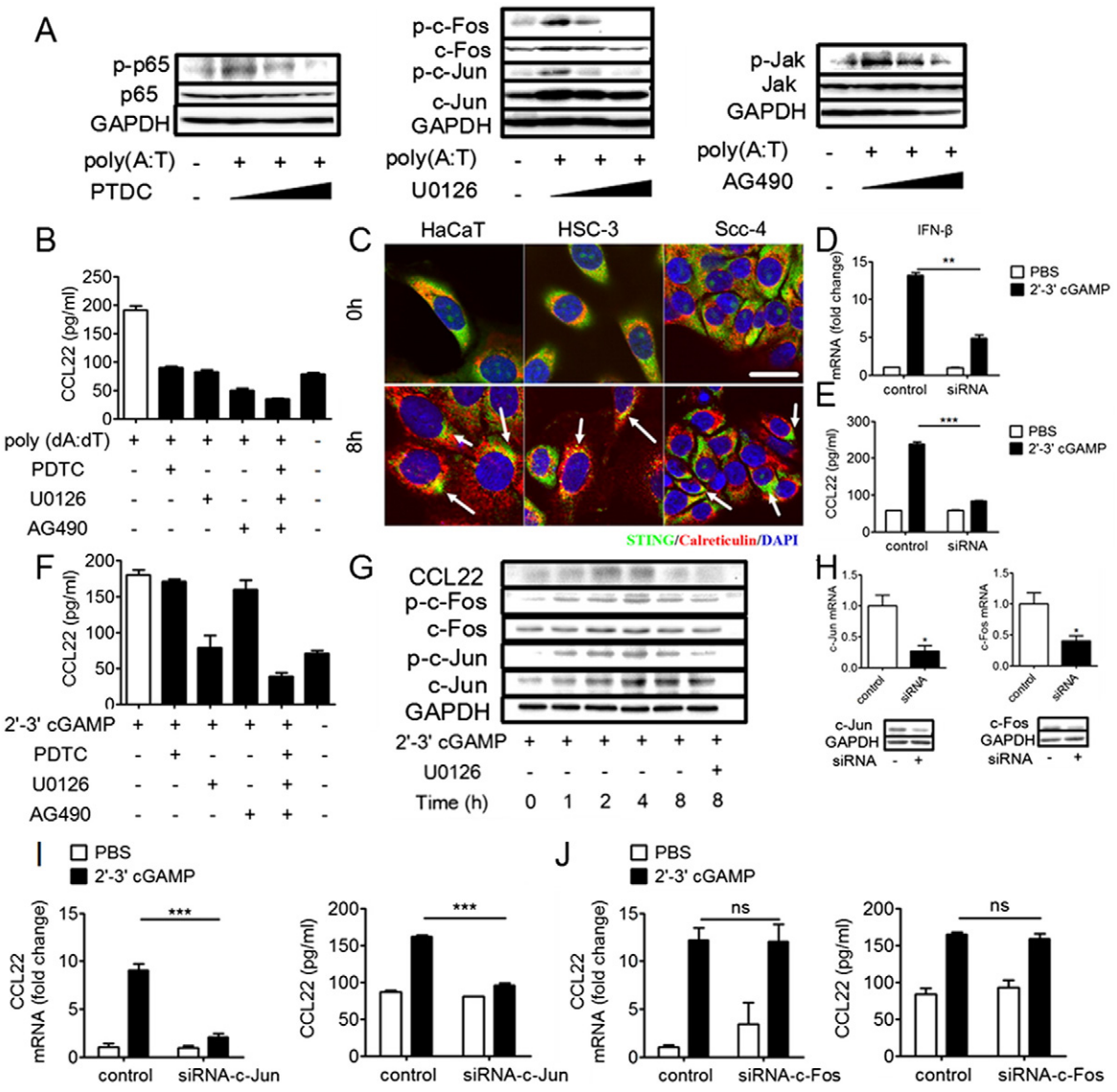

Fig. 4. STING activation up-regulates CCL22 expression via c-Jun. (A) HSC-3 cells were seeded in 6-well plates and pretreated with PTDC, U0126 or AG490 for 30 min and were then transfected with 4 μg/ml poly (dA:dT) for 5 h. Cell lysates were collected and a western blot was performed. GAPDH in the corresponding cell lysate was used as a loading control. (B) HSC-3 cells were incubated with different inhibitors and then activated STING by 4 μg/ml poly (dA:dT) for 12 h. ELISA was used to assess the impact of inhibitors on the expression of CCL22 by STING activation. (C) HaCaT, HSC-3 and Scc-4 cells were seeded in 24-well plates and transfected with 10 μg/ml 2′-3′ cGAMP for 0 h and 8 h, and then, they were immunostained with the indicated antibodies. STING is green, and calreticulin is red. Scale bar, 10 μm. (D and E) HSC-3 cells were transfected with 50 nM STING siRNA or negative control for 48 h, followed by transfection with 10 μg/ml 2′-3′ cGAMP for 12 h. The level of IFN-β and CCL22 were determined (**$P < 0.01$, ***$P < 0.001$, determined by t-test). (F) Using the same treatment in B, cells were transfected with 10 μg/ml 2′-3′ cGAMP for 12 h, and the CCL22 level was estimated by ELISA. (G) Thirty minutes after pretreatment with U0126, HSC-3 cells were transfected with 10 μg/ml 2′-3′ cGAMP for the indicated time, and whole-cell extracts were prepared for western blot. (H) The siRNA assay (negative control siRNA or c-Jun/Fos-siRNA) was performed for 24 h, and the proteins were collected after 48 h for western blot. (I and J) Q-PCR and ELISA assays were performed for the effects of c-Jun and c-Fos on the induction of CCL22 by STING activation (**P < 0.001 by t-test). Data represent the means ± s.d.

[30]. Additionally, proinflammatory cytokines, such as IL-6, CXCL10, and CCL20, are induced by STING activation to execute anti-infection immunity or autoimmunity. There have been a few studies about the role of STING in cancer, including breast cancer [25], non-small cell lung cancer (NSCLC) [8] and lymphoma [33]. For example, nuclear DNA-associated entities from dying cells were determine and uptake by dendritic cells (DCs) were found to occur in a STING-dependent manner that efficiently primed IFN-dependent $CD8^+$ T cell responses to tumor Ags and promoted antitumor responses [34]. Jirik et al. showed that STING activation by 5,6-dimethylxanthenone-4-acetic acid (DMXAA) or 2′-3′ cGAMP can mediate M2-like TAM re-education towards an M1 proinflammatory phenotype in NSCLC [8]. However, the immunosuppressive role in DNA sensing via STING has been found, and Mellor et al. showed that selective DNA uptake and sensing via STING in $CD11b^+$ dendritic cells (DCs) by apoptotic cells induced IDO and suppressed Th1 responses though Treg responses [35]. In addition, they also indicated that selective STING activation in hematopoietic cells could suppress experimental autoimmune encephalitis (EAE) by inducing dominant T cell regulatory responses via the STING/IFN/IDO pathway [10]. Another study reported that inflammation-driven skin carcinoma was mediated by activated STING [4], which suggested that STING functioned not only as a proinflammatory mediator but also as an immunosuppressive adapter. We emphasized the anti-inflammatory aspects of STING in TSCC with HPV infection.

In the present study, we observed increased STING expression in OSCC patients and cell lines. Notably, limited studies in breast cancer showed a decreased expression of STING by immunohistochemistry and Q-PCR [25]. Thus, there was a possibility that STING functioned differently in distinct types of cancer. Although investigations have found that normal tissue and cancerous tissue have significantly different

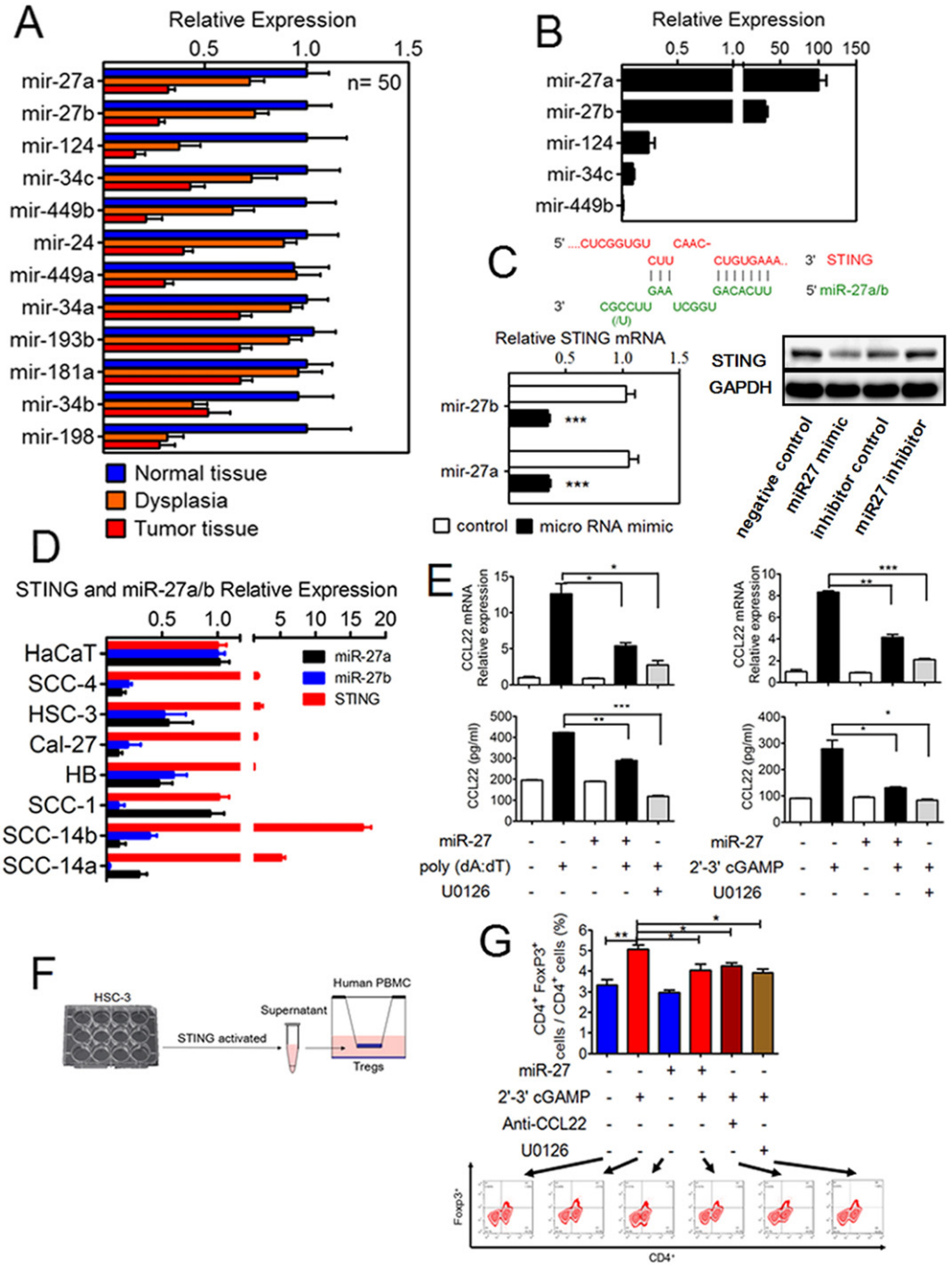

Fig. 5. miR-27 controls CCL22, which recruits Tregs by modulating STING activation. (A) microRNAs that targeted STING were measured in fresh TSCC tissue (n = 50) samples by qPCR. (B) The results are shown as different levels of five microRNAs in normal tissue. (C) Putative miR-27a/b binding sites in the 3′ UTR of STING. HSC-3 cells were transfected with 50 nM of miR-27a/b mimetic for 24 h, and the STING mRNA level was determined by qPCR and normalized to GAPDH. $^{***}P < 0.001$ (Mann Whitney test). The STING protein level was determined by Western blot. (D) The miR-27a, miR-27b and STING expression in HaCaT and TSCC cells were determined by qPCR ($^{*}P < 0.05$ by *t*-test). (E) HSC-3 cells were transfected with 20 nM miR-27 for 48 h and then incubated or not with U0126 for 30 min and transfected with 4 μg/ml poly (dA: dT) or 10 μg/ml 2′-3′ cGAMP. The supernatants were collected for ELISA. Statistical significance was analyzed by the *t*-test ($^{*}P < 0.05$, $^{**}P < 0.01$ and $^{***}P < 0.001$). (F and G) The supernatants were collected from two transfections of the indicated reagents, and 2×10^5 freshly isolated human PBMC were used for transwell assay. After 8 h of migration, cells in the lower compartment were harvested and $CD4^+CD25^+Foxp3^+$ Tregs were estimated by flow cytometry assay ($^{*}P < 0.05$, $^{**}P < 0.01$ by *t*-test). Data represent the means ± s.d.

levels of STING, the mechanism of the altered expression of STING in cancer remains unknown. Here, we illustrated a reverse relationship between STING and microRNA expression. miR-27, which regulates the gene controlling STING transcription by targeting its 3′ UTR and as well as its degradation in vitro, gradually decreased during the progression of OSCC patients. Correspondingly, the results from cell lines also showed a lower level of miR-27 in different OSCC cell lines than that in normal keratinocytes. Sunthamala et al. showed that STING and IFN-κ could be attenuated by the presence of high-risk HPV via its viral protein E2 for immune evasion in cervical cancer [21]. However, E2 proteins are expressed at early stages of the viral life cycle and have a very short half-life (full-length BPV1 E2 has a half-life of 40 min) [22]. Furthermore, our results showed that STING expression exhibited no difference between HPV^+ and HPV^- samples in tongue squamous cell carcinoma. More importantly, we found that STING functioned differently in distinct types of tumors and had a different impact

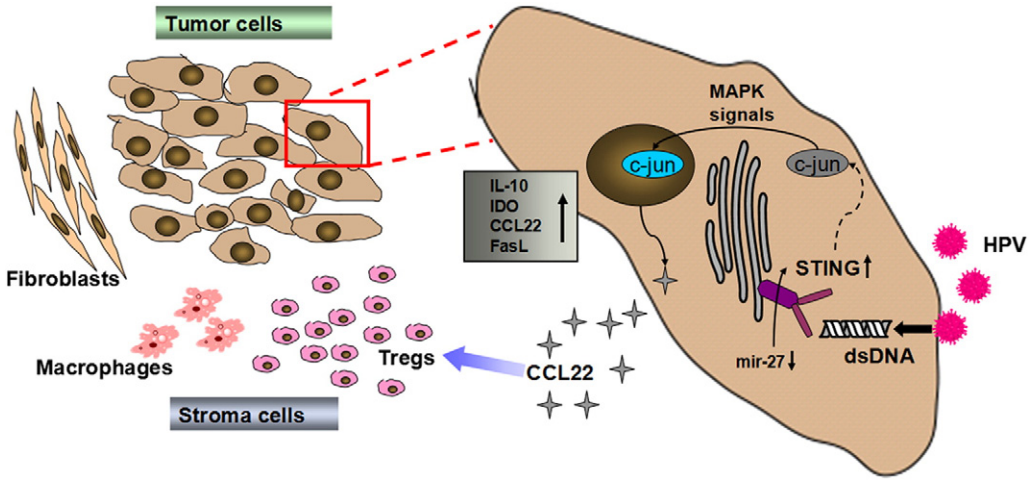

Fig. 6. Model summarizing the protumorigenic nature of STING in the microenvironment of HPV$^+$ TSCC patients. mir-27 was down-regulated during the development of TSCC, leading to the high expression of STING, which could be activated by HPV infection, and induced a series of immunosuppressive cytokines for the establishment and maintenance of the TSCC microenvironment in HPV$^+$ TSCC patients.

on cell death. Thus, we considered that HPV infection in TSCC could activate and utilize STING to participate in carcinogenesis. In fact, we noted that the activated status, as opposed to the expression, of STING might contribute to the HPV-related TSCC. In HPV$^+$ TSCC patients, STING formed cytoplasmic punctate structures around the nucleus, which was consistent with the features of STING activation, as described previously [5]. Thus, the phenomenon implicated that STING was activated by HPV in TSCC patients, suggesting that there could be a different mechanism of HPV, different from HPV integration, during tongue carcinogenesis.

Currently, more research on possible molecular mechanisms of HPV-induced carcinoma are urgently required. Potential mechanisms included the distinct sensitivity to radiation, chemotherapy or smoking habits of patients. More importantly, a HPV infection could change the status of the host immune system [13]. Many studies showed increasing levels of Foxp3 mRNA and Foxp3$^+$ regulatory T cell (Tregs) infiltration in HPV$^+$ tumors, but the mechanism of Treg infiltration in HPV$^+$ tumors has been unclear. Although both CCL22 and CCL17 were able to recruit Tregs to participate in the progression of cancer, in this study, the chemokine CCL22, but not CCL17, was remarkably up-regulated in all three cell lines by STING activation. Additionally, the clinical data supplied strong evidence that more CCL22 and Foxp3$^+$ Tregs are present in TSCC patients with HPV infection, which could supply evidence that activated STING might activate CCL22 for the recruitment of Tregs in TSCC patients.

Apart from poly(dA:dT), bacterial cyclic dinucleotides and human endogenous messenger 2′-3′cGAMP were demonstrated to effectively and directly activate STING, but the latter was a much more potent ligand of STING than other bacterial cyclic dinucleotides [3]. Although c-Jun and c-Fos play an essential role in tumorigenesis, c-Jun is more important in the development of skin and liver tumors [36]. Colburn et al. reported that transgenic mice with mutant *c-jun* impaired c-Jun/AP-1 activity and were resistant to the development of chemically induced papilloma [37]. Upon transfection of 2′-3′cGAMP into HaCaT or two TSCC cell lines, we found that STING activated the MAPK/AP-1 pathway to phosphorylate c-Jun and c-Fos, but enabled the transcription of CCL22 in a c-Jun-dependent manner and recruited Tregs. Our results highlighted the function of c-Jun in the progression of HPV$^+$ TSCC and suggested that an inhibitor of c-Jun would be a promising therapeutic drug candidate. Finally, Li et al. reported the pivotal roles of 2′-3′ cGAMP in immune adjuvant effects in a STING-dependent manner [38]. However, our results indicated that activated STING by 2′-3′ cGAMP could promote the establishment of the TSCC microenvironment by immunosuppressive cytokines, e.g., FasL, IL-10, IDO and CCL22, and recruitment of Tregs, suggesting that the immune adjuvant effects of 2′-3′cGAMP should cause us to reconsider its application, at least in HPV$^+$ TSCC patients.

5. Conclusions

In sum, these findings indicated that HPVs hijack STING to induce CCL22 to recruit Tregs and that down-regulated miR-27 amplifies the interaction among STING/CCL22/Tregs in HPV$^+$ TSCC patients, suggesting that STING is versatile in different circumstances that influence immune responses to DNA and that the STING activation pathway might be considered to be an antitumor therapeutic target in HPV-related carcinogenesis.

Author contributions

L.D., YH.N. and YY.H. designed experiments with valuable help from XF.H., GJ.D. and QG.H.. L.D. performed and analyzed data with valuable help from EL.H., TT.W.. L.D. and YY.H wrote the manuscript. XF.H and S.C. collected surgical specimens; YY.H. and YH.N. oversaw the overall project.

Supports

This work was supported by the National Natural Science Foundation of China (No. 81402238, 81072213, 81271698, 31370899), the Nanjing Medical Science & Research Project (No. YKK11039, YKK13145), Nanjing Medical Young Engineer (QRX113311), National Key Disciplines Constructional Project Funding (Since 2011), Jiangsu Provincial Clinical Medicine of Science and Technology project (Grant No. BL2012017), Nanjing Municipal Key Medical Laboratory Constructional Project Funding (Since 2012), Center of Nanjing Clinical Medicine of Tumor Project (Since 2014).

Disclose any potential conflicts of interest

The authors declare no competing financial interests.

Acknowledgments

We thank the Hospital of Stomatology, Nanjing for their helpful and essentially clinical samples.

Appendix A. Supplementary data

Supplementary data to this article can be found online at http://dx.doi.org/10.1016/j.bbadis.2015.08.011.

References

[1] H. Ishikawa, G.N. Barber, STING is an endoplasmic reticulum adaptor that facilitates innate immune signalling, Nature 455 (7213) (2008) 674–678.
[2] T. Abe, A. Harashima, T. Xia, H. Konno, K. Konno, A. Morales, et al., STING recognition of cytoplasmic DNA instigates cellular defense, Mol. Cell 50 (1) (2013) 5–15.
[3] P. Gao, M. Ascano, Y. Wu, W. Barchet, B.L. Gaffney, T. Zillinger, et al., Cyclic [G(2′,5′)pA(3′,5′)p] is the metazoan second messenger produced by DNA-activated cyclic GMP-AMP synthase, Cell 153 (5) (2013) 1094–1107.
[4] J. Ahn, T. Xia, H. Konno, K. Konno, P. Ruiz, G.N. Barber, Inflammation-driven carcinogenesis is mediated through STING, Nat. Commun. 5 (2014) 5166.
[5] T. Saitoh, N. Fujita, T. Hayashi, K. Takahara, T. Satoh, H. Lee, et al., Atg9a controls dsDNA-driven dynamic translocation of STING and the innate immune response, Proc. Natl. Acad. Sci. U. S. A. 106 (49) (2009) 20842–20846.
[6] Y. Liu, A.A. Jesus, B. Marrero, D. Yang, S.E. Ramsey, G.A. Montealegre Sanchez, et al., Activated STING in a vascular and pulmonary syndrome, N. Engl. J. Med. 371 (6) (2014) 507–518.
[7] S. Sharma, A.M. Campbell, J. Chan, S.A. Schattgen, G.M. Orlowski, R. Nayar, et al., Suppression of systemic autoimmunity by the innate immune adaptor STING, Proc. Natl. Acad. Sci. U. S. A. 112 (7) (2015) E710–717.
[8] C.M. Downey, M. Aghaei, R.A. Schwendener, F.R. Jirik, DMXAA causes tumor site-specific vascular disruption in murine non-small cell lung cancer, and like the endogenous non-canonical cyclic dinucleotide STING agonist, 2′3′-cGAMP, induces M2 macrophage repolarization, PLoS One 9 (6) (2014), e99988.
[9] Q. Zhu, S.M. Man, P. Gurung, Z. Liu, P. Vogel, M. Lamkanfi, et al., Cutting edge: STING mediates protection against colorectal tumorigenesis by governing the magnitude of intestinal inflammation, J. Immunol. 193 (10) (2014) 4779–4782.
[10] H. Lemos, L. Huang, P.R. Chandler, E. Mohamed, G.R. Souza, L. Li, et al., Activation of the STING adaptor attenuates experimental autoimmune encephalitis, J. Immunol. 192 (12) (2014) 5571–5578.
[11] E.M. de Villiers, C. Fauquet, T.R. Broker, H.U. Bernard, H. zur Hausen, Classification of papillomaviruses, Virology 324 (1) (2004) 17–27.
[12] E.R. Flores, B.L. Allen-Hoffmann, D. Lee, C.A. Sattler, P.F. Lambert, Establishment of the human papillomavirus type 16 (HPV-16) life cycle in an immortalized human foreskin keratinocyte cell line, Virology 262 (2) (1999) 344–354.
[13] R. Williams, D.W. Lee, B.D. Elzey, M.E. Anderson, B.S. Hostager, J.H. Lee, Preclinical models of HPV+ and HPV- HNSCC in mice: an immune clearance of HPV+ HNSCC, Head Neck 31 (7) (2009) 911–918.
[14] A. Nasman, M. Romanitan, C. Nordfors, N. Grun, H. Johansson, L. Hammarstedt, et al., Tumor infiltrating CD8+ and Foxp3+ lymphocytes correlate to clinical outcome and human papillomavirus (HPV) status in tonsillar cancer, PLoS One 7 (6) (2012), e38711.
[15] C. Badoual, S. Hans, N. Merillon, C. Van Ryswick, P. Ravel, N. Benhamouda, et al., PD-1-expressing tumor-infiltrating T cells are a favorable prognostic biomarker in HPV-associated head and neck cancer, Cancer Res. 73 (1) (2013) 128–138.
[16] F. Jaafar, E. Righi, V. Lindstrom, C. Linton, M. Nohadani, S. Van Noorden, et al., Correlation of CXCL12 expression and FoxP3+ cell infiltration with human papillomavirus infection and clinicopathological progression of cervical cancer, Am. J. Pathol. 175 (4) (2009) 1525–1535.
[17] M.E. Scott, Y. Ma, L. Kuzmich, A.B. Moscicki, Diminished IFN-gamma and IL-10 and elevated Foxp3 mRNA expression in the cervix are associated with CIN 2 or 3, Int. J. Cancer 124 (6) (2009) 1379–1383.
[18] R. Siegel, J. Ma, Z. Zou, A. Jemal, Cancer statistics, 2014, CA Cancer J. Clin. 64 (1) (2014) 9–29.
[19] A.J. Remmink, J.M. Walboomers, T.J. Helmerhorst, F.J. Voorhorst, L. Rozendaal, E.K. Risse, et al., The presence of persistent high-risk HPV genotypes in dysplastic cervical lesions is associated with progressive disease: natural history up to 36 months, International journal of cancer Journal international du cancer 61 (3) (1995) 306–311.
[20] W. Sun, Y. Li, L. Chen, H. Chen, F. You, X. Zhou, et al., ERIS, an endoplasmic reticulum IFN stimulator, activates innate immune signaling through dimerization, Proc. Natl. Acad. Sci. U. S. A. 106 (21) (2009) 8653–8658.
[21] N. Sunthamala, F. Thierry, S. Teissier, C. Pientong, B. Kongyingyoes, T. Tangsiriwatthana, et al., E2 proteins of high risk human papillomaviruses down-modulate STING and IFN-kappa transcription in keratinocytes, PLoS One 9 (3) (2014), e91473.
[22] A.A. McBride, The papillomavirus E2 proteins, Virology 445 (1–2) (2013) 57–79.
[23] T. Abe, A. Harashima, T. Xia, H. Konno, K. Konno, A. Morales, et al., STING recognition of cytoplasmic DNA instigates cellular defense, Molecular cell. 50 (1) (2013) 5–15.
[24] J. Petrasek, A. Iracheta-Vellve, T. Csak, A. Satishchandran, K. Kodys, E.A. Kurt-Jones, et al., STING-IRF3 pathway links endoplasmic reticulum stress with hepatocyte apoptosis in early alcoholic liver disease, Proc. Natl. Acad. Sci. U. S. A. 110 (41) (2013) 16544–16549.
[25] K. Bhatelia, A. Singh, D. Tomar, K. Singh, L. Sripada, M. Chagtoo, et al., Antiviral signaling protein MITA acts as a tumor suppressor in breast cancer by regulating NF-kappaB induced cell death, Biochim. Biophys. Acta 1842 (2) (2014) 144–153.
[26] F. Chang, S. Syrjanen, A. Tervahauta, K. Kurvinen, L. Wang, K. Syrjanen, Frequent mutations of p53 gene in oesophageal squamous cell carcinomas with and without human papillomavirus (HPV) involvement suggest the dominant role of environmental carcinogens in oesophageal carcinogenesis, Br. J. Cancer 70 (2) (1994) 346–351.
[27] C. Menetrier-Caux, M. Gobert, C. Caux, Differences in tumor regulatory T-cell localization and activation status impact patient outcome, Cancer Res. 69 (20) (2009) 7895–7898.
[28] G. Brandacher, A. Perathoner, R. Ladurner, S. Schneeberger, P. Obrist, C. Winkler, et al., Prognostic value of indoleamine 2,3-dioxygenase expression in colorectal cancer: effect on tumor-infiltrating T cells, Clin. Cancer Res. 12 (4) (2006) 1144–1151.
[29] S. Zhao, H. Wang, Y. Nie, Q. Mi, X. Chen, Y. Hou, Midkine upregulates MICA/B expression in human gastric cancer cells and decreases natural killer cell cytotoxicity, Cancer Immunol. Immunother. 61 (10) (2012) 1745–1753.
[30] H. Chen, H. Sun, F. You, W. Sun, X. Zhou, L. Chen, et al., Activation of STAT6 by STING is critical for antiviral innate immunity, Cell 147 (2) (2011) 436–446.
[31] E. Shaulian, AP-1—The Jun proteins: oncogenes or tumor suppressors in disguise? Cell. Signal. 22 (6) (2010) 894–899.
[32] Y.S. Lee, A. Dutta, MicroRNAs in cancer, Annu. Rev. Pathol. 4 (2009) 199–227.
[33] A.R. Lam, N. Le Bert, S.S. Ho, Y.J. Shen, M.L. Tang, G.M. Xiong, et al., RAE1 ligands for the NKG2D receptor are regulated by STING-dependent DNA sensor pathways in lymphoma, Cancer Res. 74 (8) (2014) 2193–2203.
[34] J. Klarquist, C.M. Hennies, M.A. Lehn, R.A. Reboulet, S. Feau, E.M. Janssen, STING-mediated DNA sensing promotes antitumor and autoimmune responses to dying cells, J. Immunol. 193 (12) (2014) 6124–6134.
[35] L. Huang, L. Li, H. Lemos, P.R. Chandler, G. Pacholczyk, B. Baban, et al., Cutting edge: DNA sensing via the STING adaptor in myeloid dendritic cells induces potent tolerogenic responses, J. Immunol. 191 (7) (2013) 3509–3513.
[36] R. Eferl, E.F. Wagner, AP-1: a double-edged sword in tumorigenesis, Nat. Rev. Cancer 3 (11) (2003) 859–868.
[37] M.R. Young, J.J. Li, M. Rincon, R.A. Flavell, B.K. Sathyanarayana, R. Hunziker, et al., Transgenic mice demonstrate AP-1 (activator protein-1) transactivation is required for tumor promotion, Proc. Natl. Acad. Sci. U. S. A. 96 (17) (1999) 9827–9832.
[38] X.D. Li, J. Wu, D. Gao, H. Wang, L. Sun, Z.J. Chen, Pivotal roles of cGAS-cGAMP signaling in antiviral defense and immune adjuvant effects, Science 341 (6152) (2013) 1390–1394.